FIELD EXPERIMENTS ON LONGSHORE SAND

TRANSPORT IN THE SURF ZONE

by

Nicholas C. Kraus<sup>1</sup>, Masahiko Isobe<sup>2</sup>, Hajime Igarashi<sup>3</sup> Tamio O. Sasaki<sup>4</sup> and Kivoshi Horikawa<sup>5</sup>

# ABSTRACT

Eight fluorescent sand tracer experiments were performed in energetic surf zones on natural beaches and on beaches near structures to measure the short-term longshore sand transport rate. Tracer of up to four distinct colors was injected on a line crossing the surf zone to investigate the on-offshore distributions of the longshore sand advection velocity and transport rate. The tracer advection velocity, v\_, and the depth of mixing into the bed, b, were determined from large numbers of cores taken in situ throughout the sampling area. The sand advection velocity and mixing depth were not constant across the surf zone, but usually exhibited a maximum either toward the shoreline or toward the breaker line, or in both regions. The local breaking wave height, H,, and horizontal current velocity in the surf zone (yielding an average longshore current velocity  $\overline{V})$  were also measured. The data were interpreted with simple dimensional arguments to give the following results: b = 0.027 H, v = 0.014  $\bar{V}$ , and the volumetric transport rate Q = 0.024 H  $_{\rm V}^2$ . Agreement was also found between the measured total longshore sand transport rate and a predictive expression due to Bagnold involving the breaking wave power and average longshore current velocity. Although the results appear reasonable and consistent, a problem remains concerning the apparent decrease in tracer advection speed alongshore recorded in most experiments at the longer sampling times.

#### INTRODUCTION 1.

The longshore sand transport rate is usually the principal factor determining erosion or accretion along a coast. If the longshore sand transport rate can be estimated, a qualitative picture may be formed of the general evolution of the coastline, including changes of the This picture can be brought to a shoreline around structures.

- M. ASCE, Senior Engineer, Nearshore Environment Research Center, 1. 1202 Famille Hongo Bldg., 1-20-6 Mukohgaoka, Tokyo, 113 Japan
- Associate Professor, Dept. of Civil Eng., Yokohama National 2. University, 156 Tokiwadai, Hodogaya-ku, Yokohama, 240 Japan
- 3. Senior Engineer, INA Civil Engineering Consulting Co., Ltd., 22-1 Suido-cho, Shinjuku-ku, Tokyo, 162 Japan
- 4. M. ASCE, Chief Engineer, Nearshore Environment Research Center, 1-20-6 Mukohgaoka, Bunkyo-ku, Tokyo, 113 Japan 5. M. ASCE, Professor, Dept. of Civil Eng., University of Tokyo,
- 7-3-1 Hongo, Bunkyo-ku, Tokyo, 113 Japan

quantitative level with numerical models of shoreline change. Such models require a predictive formula for the total longshore transport rate in terms of the average wave and current conditions. Because structures extend across the nearshore zone, a predictive expression for not only the total transport rate, but also the distribution of the longshore transport rate, is required to accurately describe changes which occur in the sea bottom and shoreline in the vicinity of such structures.

Only a limited number of field measurements of the longshore sand transport rate have been attempted. For example, Bruno et al. (1980) discuss 56 field data points. Most of these measurements may be rejected for violating certain criteria or because of experimental uncertainties (Greer and Madsen, 1978; Bruno et al., ibid).

The goals of our sand tracer field experiment program were 1) to obtain data for evaluating predictive expressions for the short-term (order of hours) total longshore sand transport rate, 2) to obtain some knowledge of the distribution of the transport across the surf zone, and 3) to determine the applicability and limitations of tracer techniques applied to real surf zones. Five of the experiments were part of a comprehensive multi-institutional cooperative field investigation conducted in Japan from 1978 to 1982.

# 2. BACKGROUND OF EXPERIMENTS

#### 2.1 Study Sites



Fig. 1 Location of experiment sites.

The experiments were performed on four beaches: Ajigaura, Oarai, Hirono and Shimokita, facing the Pacific Ocean on the east coast of Japan (Fig. 1). The experiments are referred to by the beach name, and year, if necessary, except for the two experiments at Hirono per-Shimokita formed on consecutive days in 1980, termed Hirono-1 and Hirono-2. The experiments at Oarai were performed to investigate the influence of structures on the waves, current, and sediment transport. Table 1 gives the basic characteristics and brief descriptions of the sites.

> The tidal range on these beaches is rather small, about 1 m. As much as possible, the experiments were performed during or near an inflection point in the tide to minimize its effect. The tide is considered to have had negligible influence except possibly for a rising tide occurring near the end of Oarai 81.

sites.	
experiment	
beach	
of	
Characteristics	
TABLE 1	

Experiment	Median grain size d <sub>50</sub> (mm)	Sorting coef. (d <sub>75</sub> /d <sub>25</sub> ) <sup>1/2</sup>	Specific gravity	Composition	Nearshore beach slope	Comments
AJIGAURA 78	0.23	1.1 (estimated)	2.65	quartz	1/50 to 1/70	Coast is 9 km long with no significant structures;
AJIGAURA 79	0.27	1.1 (estimated)	2.65	quartz	1/50 to 1/70	Algaura /8 perrormed near south headland, Ajigaura 79 performed near middle of coast
SHIMOKITA	0.18	1.06	3.13	guartz heavy minerals	1/40 to 1/60	Long coast (38 km) with uniform contours
HIRONO - 1	0.59	1.69	2.67	quartz sand & pebbles	1/10	Pocket beach
HIRONO - 2	0.59	1.69	2.67	quartz sand & pebbles	1/10	Same location as Hirono l
OARAI 80	0.25	1.09	2.79	guartz	1/50 to 1/70	Near large groin and behind harbor breakwater
OARAI 81	0.24	1.16	2.79	guartz	1/50 to 1/70	Same location as Oarai 80
OARAI 82	0.25	1.05	2.79	guartz	1/30 to 1/40	Behind harbor breakwater and 2 km south of Oarai 80; beach slope steep due to erosion

arrangements.
experiment
of
Summary
TABLE 2

ITEM	AJIGAURA	URA	SHIMOKITA	HIRON	HIRONO	OARAI	OARAI	OARAI
	1978	1979	1979	13 Nov	au 14 Nov	1980	1981	1982
Longshore stations	12	13	17	18	18	18	18	20
Grid length alongshore	130; 210	130	255	300	200	130	175	100
Offshore stations	9	7 & 9	8	5	5	7	6	12
Offshore spacing (m)	10	7.5	10	4	4	8	10	ñ
Width of surf zone (m)	60	52.5	80	20	20	56	06	36
<u>Spatial Samplings</u>	4	2	m	3	e	2	2	2
Start of sampling after injection (min)	15, 30 70, 120	30, 120	30 120, 180	<b>4</b> 5 105, 165	60 120, 180	90, 180	90, 180	60, 180
Temporal Samplings	ı	13	12	1	16	19	30	1
Sampling interval (min)	ı	15	15	'	15	15	10	I
Number of lines	ı	7	а	ı	1	1	I	I
Distance from injec. line to sampling line (m)	ı J	10, 20	10, 20	ı	ø	15	15	ı
Number of tracer colors	5		2	1		3	3	4
Outer Colors Mid Inner	green - ređ	orange red green	green - red	ređ	- green	orange red green	orange red green	orange blue, red green
Amount of tracer inj'd for each color (kgf)	100,100	100,100,100	150,150	50	60	50, 40, 40	27,27,27	1.5 Per color
Wave measurement*	stereo photos direct sighting	PWG 16mm	16mm	16mm	16mm	16 mm PWG;CWG	CWG; PWG 16mm	16 mm
Current measurement*	floats	EMCM (5) floats	EMCM (3) floats	EMCM (2) floats	EMCM (3) floats	EMCM (3) floats	EMCM (2) floats	EMCM (3) floats
*) PWG (CWG) = pressure (capacitance) wave gage; 16mm = 16mm memo-motion camera; BWCM = electromagnetic current meter (numbers in parenthesis give number of meters used)	capacitance) wav current meter	ve gage; l6mm (numbers in pa:	= 16mm memo-r renthesis give	motion camera e number of m	17 . leters used)			

COASTAL ENGINEERING-1982

## 2.2 Experiment Design

A schematic of the general experimental arrangement is shown in Fig. 2. A summary of the arrangements and sampling schedules of all eight experiments is given in Table 2. Four features distinguish these experiments from previously reported ones. These are:

i) Multicolor tracer injections were often applied to measure the distribution of the longshore transport rate, and to separate longshore and on-offshore effects.

ii) Core samples were taken in situ at all times and at all locations. Before 1980, hand-held wedge-shaped PVC tubes were used for sampling. From 1980, a special coring device was used (Kraus et al., 1981).

iii) Two to four samplings by the spatial integration method were made in all experiments. In addition, sampling by the time integration method was made in four of those experiments.

iv) Three experiments were performed near structures.

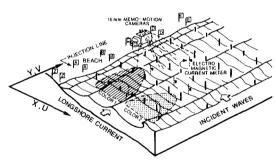


Fig. 2 Schematic of multicolor tracer experiments, and axes convention.

tracer. Komar (1969) extensively used the SIM. Inman et al. (1980) performed the SIM and TIM in combination as we did in four experiments. In our experiments a one-time injection of tracer was used. Duane and James (1980) used a continuous injection method. These and other sampling methods have been described by Lean and Crickmore (1963) for tracer techniques applied to transport in rivers.

Sand from the area of the beach face and tagged with one of four fluorscent colors was presoaked in a solution of water and detergent and injected as a line source. We have found that injections in amounts of 1 kgf/m on-offshore yield acceptable results. If the amount is too large, the counting time increases due to high concentrations; if too little tracer is injected, statistically significant amounts will not be recovered. Normally, injection was made by carefully cutting open small bags of tracer held on the surf zone bottom. In Oarai 82 the tracer was injected to a depth of 5 cm by operating the core samplers "in reverse": no appreciable difference was noted.

Two sampling methods were used. The spatial integration method (SIM) involves near-simultaneous sampling on a two-dimensional grid to determine the location of the tracer center of mass. The time integration method (TIM) involves frequent sampling on a line crossing the surf zone and down-current from the injection line to record passage of the

The samples were segmented to a certain nominal depth, typically 6, 10 or 14 cm, depending on the results of a preliminary analysis of the mixing depth. In three experiments (Ajigaura 78, Ajigaura 79, and Oarai 82), all samples were processed as core samples (yielding on the order of a thousand segments of thickness 1 or 2 cm per experiment). In the other experiments, only samples on certain longshore and on-offshore lines were finely segmented in 1- or 2-cm lengths. The remainder were processed in 4- or 6-cm segments and treated as grab samples in the analysis. These data sets of several hundred to a few thousand segments per experiment provide a detailed picture of the horizontal and vertical movement of the tracer over a wide area of the surf zone.

The tracer was counted by hand under ultraviolet light. Concentrations were expressed as a number per unit volume of sample, in effect the number of grains per centimeter in the bed for a fixed sampler surface area. A spectrofluoroscopic counting method was devised for high concentrations (Farinato and Kraus, 1981). However, the method was not implemented because of the necessity for a chemical technician.

It was decided to make local wave measurements to avoid introducing uncertainties such as might arise from refracting waves from deep water, use of a breaking criterion, complications of diffraction from structures, etc. The wave field was measured by capacitance wave gages and by filming the water surface elevation at poles with 16mm cameras from a high elevation on the beach (Fig. 2; Table 2). The camera system is very reliable and has provided otherwise unobtainable data on wave characteristics in the nearshore zone (Hotta and Mizuguchi, 1980).

Except for Ajigaura 78, the current was measured with electromagnetic current meters, usually at three points on a line crossing the surf zone and near the injection line. Ideally, measurements should be made in the swash zone, in the midsurf zone, and just inside the breaker line. However, it is difficult to record in shallow water because the meter sensor is often exposed. Therefore the instruments usually had to be placed in the mid- and outer surf zone. The sensors of these twocomponent current meters were positioned 10 to 50 cm from the bottom.

# 3. METHOD OF ANALYSIS

#### 3.1 General

Experiments based on a one-time injection of tracer require measurement of two quantities: 1) the sand advection velocity in the longshore direction,  $v_{a}$ , determined from the movement of the center of mass of the tracer and 2) the depth of mixing, b, determined from cores of material removed from the bed. The total volumetric rate of sand transport in the longshore direction, Q, is calculated by forming the product of these quantities with the width through which the transport takes place, usually the width of the surf zone,  $x_h$ :

$$Q = v_a b x_b \tag{1}$$

A conceptual model with the conditions and time scales for which Eq. 1 is expected to hold is given in Kraus et al. (1981).

Both the advection velocity and depth of mixing may vary across the surf zone. It is therefore appropriate to consider the volumetric transport rate per unit width of the surf zone, q, given by

q = v<sub>a</sub> b

(2)

This quantity depends only on the sediment response. In multicolor tracer experiments, if the tracer remains localized on-offshore as it moves alongshore, q gives an estimate of the distribution of the transport rate on-offshore.

# 3.2 Tracer Center of Mass and Advection Velocity (SIM)

An element of the grand concentration array containing the number of recovered tracer grains per unit volume (or per centimeter in the bed) is represented by N(c,i,j,k,n), where the index c denotes the tracer color, i denotes the offshore grid coordinate, j denotes the longshore grid coordinate, k denotes the segment coordinate and n denotes the sampling time. In some experiments there were sufficient numbers of divers to sample the grid rapidly. Then the samples were taken semi-randomly proceeding from the injection line. In other experiments two teams of divers sampled simultaneously on their respective lines on-offshore. In this case a sampling took about 20 to 30 min, depending on the size of the grid and the wave conditions.

Formulae for calculating the tracer advection velocity are derived in the Appendix. In application, the notation is simplified by the following conventions: the offshore limit is assumed to be the station at the breaker line, the symbol  $N_{i,j}$  represents a sum over k of all segments at the location (i, j), and the symbol c for color and summations over color are suppressed.

The longshore position of the tracer center of mass is given by

$$\mathbf{Y} = \mathbf{t}_{0} \sum_{\mathbf{i},\mathbf{j}} \frac{\mathbf{y}_{\mathbf{j}}}{\mathbf{t}_{\mathbf{j}}} \mathbf{N}_{\mathbf{i},\mathbf{j}} \left(1 - \frac{\mathbf{y}_{\mathbf{j}}}{\mathbf{t}_{\mathbf{j}}} \frac{\Delta \mathbf{t}_{\mathbf{j}}}{\Delta \mathbf{y}_{\mathbf{j}}}\right) \Delta \mathbf{y}_{\mathbf{j}} / \sum_{\mathbf{i},\mathbf{j}} \mathbf{N}_{\mathbf{i},\mathbf{j}} \left(1 - \frac{\mathbf{y}_{\mathbf{j}}}{\mathbf{t}_{\mathbf{j}}} \frac{\Delta \mathbf{t}_{\mathbf{j}}}{\Delta \mathbf{y}_{\mathbf{j}}}\right) \Delta \mathbf{y}_{\mathbf{j}}$$
(3)

The advection velocity is simply  $v_a = Y/t_o$ , where  $t_o$  is taken to be the time of sampling on the injection line. The position of the tracer center of mass on-offshore was calculated by the simple approximation

$$X = \sum_{i,j} x_i N_{i,j} \Delta y_j / \sum_{i,j} N_{i,j} \Delta y_j$$
(4)

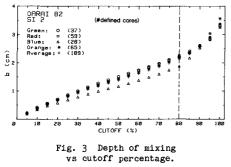
#### 3.3 Depth of Mixing

The depth of tracer mixing is a matter of definition. It has been variously defined as the depth of greatest burial (Komar, 1969; Gaughan, 1978) or as one of several kinds of concentration- or depth-weighted averages (Crickmore, 1967; Gaughan, 1978; Inman et al., 1980). In our experiments, most of the tagged sand in the cores was typically contained in the upper 6 cm, but frequently some grains were found as deep as 20 cm. This makes a maximum depth or depth-weighted definition of b either unrealistic or highly subjective. Under steady waves and currents, a developing core concentration profile should have a maximum in the surface layer and decrease monotonically with depth. At equilibrium, the tracer should be uniformly distributed from the surface to some maximum depth. In reality, conditions are not steady and samples often exhibit one or more positive concentration gradients with depth, indicating the occurrence of two or more high energy turbulence events, or that local erosion or accretion took place.

We developed a definition of the depth of mixing with a variable parameter, the percentage of tracer contained in a core to a certain depth, in order to investigate the effect produced by the various irregular concentration profiles (Kraus et al., 1980, 1981). Within any core segment (typically of thickness 1 or 2 cm), the tagged grain concentration is assumed to be uniformly distributed. Then for each core, a local mixing depth is calculated which includes a specified percentage of the total tagged grains of a particular color. The mixing depth, b, is then defined as a simple average of a particular subset of local mixing depths. In previous work we used a concentration-weighted average but, because recovered numbers of tagged grains in a core can vary over two or three orders of magnitude, a simple average was later adopted. This procedure was strengthened with a criterion requiring that at least one segment contain more than a specified number of grains. After examining thousands of core profiles from several experiments, the minimum cutoff was set at 5 grain/cm. Assuming that this criterion eliminates statistically unreliable cores having a high "noise" content, the cores accepted for analysis can then be considered of equal weight.

An additional criterion was imposed in an attempt to remove cores suspected of being contaminated by erosional or accretionary events. Cores were rejected if a segment with no tagged grains appeared between segments containing 50% of the tracer in the upper part of the core. This criterion reduced values of b by approximately 25% from those calculated previously.

The effect of the cutoff percentage on the average mixing depth was examined. It was found that a linear relation is maintained to a certain cutoff percentage, after which the relation deviates significantly from linearity. An example is shown in Fig. 3 for Oarai 82. This



result indicates that uniformity in mixing exists to a certain depth, after which the amount of tracer rapidly tails off. Wе found that a cutoff percentage of 80% was suitable for all the experiments, similarly to Kraus et al. (1980, 1981). A complete description of the experimental results and analysis of the depth of mixing is in preparation (Kraus and Isobe, in prep.)

### 4. RESULTS

## 4.1 Budget of Tracer

An estimate of the total number of tracer grains transported over the sampling grid can be made by assuming that the number of grains recovered at a site is representative of the surrounding area. Since the tracer grains in the samples were counted to their point of extinction, the calculation can be made without reference to the depth of mixing. Knowledge of the number of tracer grains per unit weight of the injected tracer allows comparison between the number of grains injected and the number accounted for by the sampling.

Although this procedure is straightforward in principle, in practice one cannot be certain of the absolute value of the calculated recovered amount because of the difficulty in counting the number of tagged grains in, say, 1 gf of tracer. Therefore, the acceptability of the measurements was judged by comparing the relative amounts recovered at the different (SIM) samplings. If a significantly smaller amount of tracer was recovered compared to other samplings, that sampling was considered unreliable. Most of the rejected measurements were from the earlier sampling times. This is attributed to the fact that the grid was relatively coarse with respect to movement of the tracer at the earlier times. Results associated with the earlier samplings were therefore not included in correlations employing waves and current.

## 4.2 Sediment Response

The principal results of the sediment response for the SIM experiments are summarized in Table 3. Background data on the average wave and current conditions are summarized in Table 4. In what follows,  $(H_b)_{1/3}$  will be written as  $H_b$ . Values for the current in Table 4 are averages over the elapsed time of the final spatial sampling.

# (1) Position of tracer center of mass (X, Y)

In Table 3, the notation "outer, mid, inner" refers to the relative positions of the different colors of tracer. It is seen from the Xentries that the tracer remained localized on-offshore (with the exception of Hirono-1 discussed in Subsection (4) below), even though the shore-normal component of the current was usually directed offshore (Table 4). An explanation for this might be that the transport produced by the steady offshore current in the surf zone, which we and co-workers have found to exist in the great majority of our field experiments, is balanced by the transport resulting from the large onshore component of wave orbital velocity due to wave asymmetry.

The purpose of performing two or more spatial samplings was to eliminate start-up or equilibration effects. We wished to check the reproducibility of the results by reference back to a previous position of the center of mass, not necessarily the injection line. Unfortunately, as can be seen from the Y-values in Table 3, for most experiments a large translation of the tracer alongshore was recorded at the earliest sampling and then very little movement took place in the later samplings. This result may also be attributed to the relative grid coarseness at the early samplings.

$ \begin{array}{cccccccccccccccccccccccccccccccccccc$			DILA 19	AJIGAURA 1978		AJIGAURA 1979	AURA 79	ER [	SHIMOKITA 1979			HIRONO-1 11/13/80	- 0	н <del>-</del>	HERONO-2 11/14/80	ŅĢ	OARAI 1980	AI 80	0AR 19	OARAI 1981	OARAI 1982	ARAI 1982
$ \begin{array}{cccccccccccccccccccccccccccccccccccc$		5	8	2	120	ñ	120	õ	120	180		105	165	60	120	180	8	180	8	180	60	180
$\begin{array}{cccccccccccccccccccccccccccccccccccc$	x/x																					
$\begin{array}{cccccccccccccccccccccccccccccccccccc$	outer	ı	64.0	0.50	0.42	0.74	0.82	0.60	0.72	0.75		,	(		ľ	,	i c	13 0	0 10	1.4		19
$\begin{array}{cccccccccccccccccccccccccccccccccccc$	tid	ł	1	ı	1	0.66	0.77	۲	; ,	<u>}</u> '	0.72	0.32	0.23	0.56	0.39	0.45	0.36	0.41	0.42	0.50	0.57	0.58
$\begin{array}{cccccccccccccccccccccccccccccccccccc$	aid Tanga	,	1	۱. •	• ;	ı ¦	÷ ،	•	ċ		ı	·	ı	،	ī	,	' ı	1	ı	•	0.32	0.31
$\begin{array}{cccccccccccccccccccccccccccccccccccc$	THINK	•	2.5	1.32	c:	0.30	0.44	0.44	0.43	0.45	•	,	•	۰	1	•	0.31	0.29	0.21	0.24	0.28	0.20
$\begin{array}{cccccccccccccccccccccccccccccccccccc$	(ш)																					
$\begin{array}{cccccccccccccccccccccccccccccccccccc$	uter	1	- FC	5	3 66	• ;	, ,	•	000	, ,							•		:			
$\begin{array}{cccccccccccccccccccccccccccccccccccc$	nid		· · ·	, , ,	••••	12.5	5.45 8 8 1	10.9	6.02	<u>.</u>			- yc			۽ '	- 1	12.7	8 20 20	39.7	53.3	52.0
$ \begin{array}{cccccccccccccccccccccccccccccccccccc$	ld	1	•		,	} '		•											0.0		2.12	1
$\begin{array}{cccccccccccccccccccccccccccccccccccc$	nner	ı	26.3	16.4	27.6	34.7	47.6	32.6	22.0	38.6							25.3		3.4	12.6	28.1	31.9
$\begin{array}{cccccccccccccccccccccccccccccccccccc$	o (cm)																					
$\begin{array}{cccccccccccccccccccccccccccccccccccc$	outer	7.5	3.7	C.4	5	0.0	0 0	П С	и с	5						a r	,	c		, ,		
$\begin{array}{cccccccccccccccccccccccccccccccccccc$	pju		5	5	8.6	5.0		2.0			ı		2.7	2	4.6	 	, - , -	, c		•		
$\begin{array}{cccccccccccccccccccccccccccccccccccc$	bid			•		•	ì			; ·	,	ı	۶۰	; '	į,	;,	5, 1	· ·	; ·	ç.	, <u>r</u>	
$\begin{array}{cccccccccccccccccccccccccccccccccccc$	nner	3.4	е•е	3.8	0°4	2.7	3.9	2	1.2	2.2	3.7	5.4 †	а.4	1.6	2.3	2.0	 	3.2	2.0	2.1		2.4
$\begin{array}{cccccccccccccccccccccccccccccccccccc$	iverage	3.4	3.5	3.8	¢.3	2.6	3.2	<b>1.5</b>	2.0	2.9	3.7	4.5	3.0	2.1	2.9	3.0	2.6	2.5	2.3	2.5	1.6	2.1
$\begin{array}{cccccccccccccccccccccccccccccccccccc$	txp't avg.		m	80		2.	6		2.1			3.7			2.7		2.	5	2.4	7	1.9	
$\begin{array}{cccccccccccccccccccccccccccccccccccc$	a (ma/s)																					
$\frac{1}{3(s/m)} = \frac{1}{100} + \frac$	outer	ł	17.4	5.2	4.7	23.3	5.5	10.5	2.9	1.4	,	1	•	ı	ı	,	2.1	1.2	6.1	3.7	6.5	5.0
$\frac{11.6}{7(s/m)} = \frac{14.6}{1.5} \cdot \frac{3}{1.3} \cdot \frac{3}{15.5} \cdot \frac{5}{1.4} \cdot \frac{3}{13.1} \cdot \frac{3}{3.6} \cdot \frac{5}{2.5} \cdot \frac{5}{6.3} \cdot \frac{3}{0.4} \cdot \frac{2}{2.7} \cdot \frac{3}{3.5} \cdot \frac{2}{2.7} \cdot \frac{3}{3.7} \cdot \frac{7}{3.7} \cdot \frac{7}{$	D La	ı	١	ı	ı	7.0	2.6	1	•	1	6.3	0.4	2.7	3.5	2.7	3.7	9.4	8.1	2.8	9.1		
$\begin{array}{cccccccccccccccccccccccccccccccccccc$	bid	ı	۱.	١	• ;	•	۰.	۱,	ı	۰,	ı	ï	ı	ı	•	ı	٠	ı	ı	ı	6.2	3.0
7/s/m) - 62.3 20.0 20.6 51.8 15.8 18.0 6.9 4.5 - 23.2 1.6 8.2 7.1 7.8 11.0 1 20.4 7.5 23.2 1.6 8.2 7.1 7.8 11.0 1 - 49.2 14.1 14.8 51.6 55.7 28.4 5.1 9.2	average	• •	16.0	5.9° 7	0 m 7 #	19.5	0.0 0.1	8.4	- 0.8	5.5 5.5	- 9	- <b>7</b>	- 2.7	3.5	- 2-7	3.7	4.7 8.8	2.8	0.6 2.5	1.2	2.8 . 6	а. •
- 62.3 20.0 20.6 51.8 15.8 18.0 6.9 4.5	q (10 <sup>-5 m3</sup> /s	(a						•												:	2	
20.4 7.5 23.2 1.6 8.2 7.1 7.8 11.0 - 19.2 14.1 14.8 51.6 25.7 28.4 5.1 9.2	outer	ı	62.3	20.0	20.6	51.8	15.8	18.0	6.9	4.5	ı	ı	ł	ı	ı	í	4.7	2.4	15.4	•	10.7	1.7
ar - 49.2 14.1 14.8 51.6 25.7 28.4 5.1 9.2	bid	ı	۱	ı	•	20.4	7.5	ı	ı	٠	23.2	1.6	8.2	7.1	7.8	11.0	10.7	3.9	6.9	3.7	12.8	5
- #9.2 1#.1 1#.8 51.6 25.7 28.# 5.1 9.2	D10	ı	•	ı.		ı	ı	ı	•	•		,	•	•	1	,	ı	,	•		9.1	5.3
	inner	۱	49.2	14.1	14.8	51.6	25.7	28.4	5.1	<b>9.</b> 2	ı	1	ı	۱	ı	ı	14.6	8.8	1.2		13.2	7.1
		• 1				-	2		2	2	r		Ī	<u>.</u>	-	2.2	<b>B</b> •0	0.2	2	n		

\* Per cent recovered low in relative sense

•									
ITEM		AJI 1978	GAURA 1979	SHIMORITA 1979		D (1980) 11/14	1980	OARAI 1981	1982
Breaking Waves									
depth h <sub>b</sub>	(cm)	90	130	110	190	120	100	140	100
height (Hb) 1/3	( <b>c</b> m)	98	110	63	161	100	100	111	80
surf. elev. $(\eta_b)_{rms}^{1/3}$	(cm)	20	28	17	37	24	24	26	21
period (Tb) 1/3	(8)	9.0	6.5	4.9	8.7	8.4	10.2	6.1	7.5
angle 8 <sup>b</sup> b	(deg)	6	2	6	2	3	-8	6	4
Longshore Current									
v (cm/s	)								
meter 1	outer	53*	31	18	22	14	6	27	
2	mid	52*	34	28	19	17	26	7	
3	inner	45*	37	25	**	15	**	**	
4	inner	**	28	**	**	**	**	**	*1
6	miđ	**	34	**	**	**	**	**	**
Offshore Current									
ū (ст./в	)								
meter 1	outer	**	8	25	15	5	-2	3	4
2	mid	**	11	25	26	24	~6	1	19
3	inner	**	13	23	**	5	**	**	13
4	inner	**	9	**	**	**	**	**	**
6	mid	**	24	**	**	**	**	**	**
* Current measured	by float	з.							

TABLE 4 Average wave and current conditions during experiments.

# (2) Depth of mixing (b)

The depth of mixing was calculated for each color of tracer according to the procedure discussed in the previous section. In Table 3, it is observed that the depth of mixing tended to increase slightly with time. In some experiments a bimodal distribution in b is noted whereas in other experiments a maximum is found either near the shoreline or near the breaker line. An unambiguous maximum was not found in the midsurf zone. Mechanical stirring of the bottom, which would result in large concentrations of suspended sediment and greater mixing depths, is expected under certain breaking waves and in the swash zone. There is normally no similar stirring process in the middle of the surf zone.

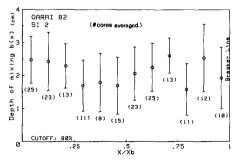
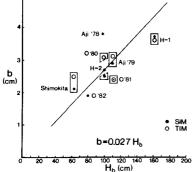


Fig. 4 On-offshore distribution of the depth of mixing (Oarai 82).

Figure 4 plots the onoffshore distribution of the mixing depth for the second spatial sampling at Oarai 82. The bars are two standard deviations. This representative result shows that there is great variability in the mixing depth at any one location. An average mixing depth calculated from a small number of cores would therefore be unreliable. It is seen that the mixing depth had maxima in the swash zone and near the breaker line in this experiment.



It is reasonable to assume that the mixing depth is proportional to the breaking wave height. The experiment-average values of b have been plotted against the significant breaking wave height in Fig. 5. It should be emphasized that these values are each the average of many cores. A best-fit straight line through the origin gives

$$b = 0.027 H_{b}$$
 (5)

Equation 5 pertains to mixing depths resulting from steady waves, with minimal influence of the tide.

Fig. 5 Depth of mixing.

(3) Tracer advection velocity  $(v_a)$ 

If the transport is fully developed, we expect the sand advection velocity to be proportional to the mean longshore current. Advection velocities for elapsed times greater than 60 min (SIM) are plotted against the average current over that time in Fig. 6. Although there is considerable scatter, by fitting a line through the origin, we get

v = 0.014 V

(6)

The advection velocity determined by the TIM was always greater than that from the SIM. For the two experiments in which the TIM was performed on two distinct lines (Ajigaura 79 and Shimokita 79), the calculated advection velocity was essentially proportional to the distance from the injection line to the sampling line.

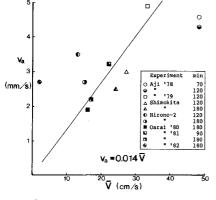


Fig. 6 Sand advection velocity.

To understand these results, the numbers of tagged grains found on the temporal sampling lines were plotted as a function of time. The numbers did not systematically increase and then decrease through the duration of the sampling as one would expect, but rather remained almost constant. Large numbers of grains were thus recovered both at the earlier and later samplings. The appearance of large numbers of grains at the early samplings produces a high transport rate because the TIM gives more weight to early times (Eq. A-5). The fact that large numbers were recovered at later

sampling times indicates that the tracer center of mass did not pass the sampling line, a result in contradiction to values computed with the SIM. Inman et al. (1980) also report higher advection velocities for the TIM. It appears that the TIM sampling line should have been located closer to the injection line (say, 5m), but in view of the SIM results this requirement is puzzling.

(4) On-offshore distribution of the transport rate (q)

The entries for q in Table 3 show that the distribution of the transport rate in the field does not take a universal form. The multicolor tracer experiments gave a constant distribution for Shimokita, a distribution with a maximum toward the breaker line for Oarai 81 and Ajigaura 78, a definite bimodal distribution for Ajigaura 79, and a distribution with a maximum toward the inner surf zone for Oarai 80 and Oarai 82. The diversity in distributions can be explained by considering the combined effects of the current and the mode of transport (bed load or suspended load).

It is the authors' experience that the typical longshore current profile in the field is rather flat across most of the surf zone, unlike the velocity distribution observed and predicted for a uniformly sloping (laboratory) beach, which is well peaked in the midsurf region. A flat profile was found in Ajigaura 79 and Shimokita (Table 4). Another such field example was reported by Kraus and Sasaki (1979). A broad flat longshore current profile may be explained to be a result of the steptype bottom which is usually found on gently sloping beaches (Mizuguchi and Horikawa, 1978). That is, waves can break, reform, and break again on nonplanar beaches. In the vicinity of structures, the longshore variation in wave height due to diffraction may also considerably alter the current distribution. For the beach at Oarai, the variation in breaking wave height produced by the harbor breakwater has been measured, calculated, and related to the sediment transport and shoreline change using a numerical model of shoreline evolution (Kraus and Harikai, 1983). Other three-dimensional processes on a real beach will also alter the idealized longshore current distribution (Sasaki, 1980).

Therefore, there is no reason to expect a well-defined peak in the longshore transport in the field on the basis of theoretical considerations of the longshore current on a plane beach (Komar, 1977), or as measured in laboratory experiments (Sawaragi and Deguchi, 1978; Tsuchiya, 1982). It does seem reasonable that the longshore transport would exhibit a peak, however, in regions where suspended load transport is high (swash zone and breaker zone under certain conditions). This approach must be refined by considering the criteria for the existence of a swash zone, and the breaker type (e.g., as done by Kamphuis and Readshaw, 1978).

The surf zones encountered for Hirono-1 and Oarai 82 illustrate this point. During Hirono-1, high waves arrived on this steep beach as collapsing breakers and continued to run up as a turbulent bore. The entire surf zone consisted of intense swash which moved up the beach in expanding circular "wavelets". Near the shoreline the tracer was observed to move either in the direction of the mean longshore current or opposite to it, depending on the direction of the expanding circular wavelet of the bore at a given location. Under these conditions sand moved rapidly onshore with very little net longshore movement despite the strong current recorded in the deeper region near the breaker line.

In Oarai 82, waves broke mainly as spilling breakers. Little wave energy was expended at the breaker line. The surf zone was unusually turbulent and clouds of suspended sediment were seen at all locations. Table 3 shows that the advection velocity and transport were essentially constant in this four-color experiment, except near the shoreline, where the longshore current was relatively stronger. The slowly rising tide moved the most landward-injected tracer onshore.

# (5) Total transport rate (Q; I)

1

The total transport rates are given in the last row of Table 3. They were calculated by averaging over the products of  $v_{\rm A}$  and b for the respective regions and then multiplying by the width of the surf zone. In order to relate the transport rate to the wave and current conditions, Eqs. 5 and 6 were substituted into Eq. 1, and a planar beach slope was assumed, for which  $x_{\rm b}$  =  $h_{\rm b}/(\tan\beta$  =  $H_{\rm b}/(\gamma_{\rm b}\tan\beta)$ , where  $\tan\beta$  is the beach slope and  $\gamma_{\rm b}$  is the ratio of wave height to water depth at the breaking point. An empirical formula is thus obtained,

$$Q = \frac{3.8 \ 10^{-4}}{\gamma_b \ \tan\beta} \ H_b^2 \ \overline{v}$$
(7)

which is dimensionally correct. For a given wave height and average longshore current, Eq. 7 states that the transport should be greater on a more gently sloping (wider) beach. The data are plotted in Fig. 7. The dependence of Q on the beach slope is given some support by comparing results for Shimokita (gentle slope) and Hirono (steep slope).

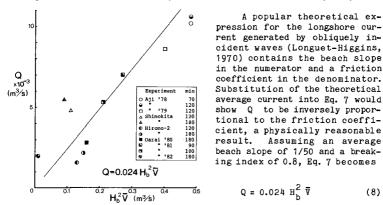


Fig. 7 Volumetric transport rate.

The experimental results for the mixing depth and advection velocity have thus indicated that the combination  $\mathrm{H}_{\mathrm{D}}^{2}\,\overline{\mathrm{V}}$  is a natural quantity on which the total volumetric transport rate should depend. In Fig. 7, the straight line is given by Eq. 8, which also gives the best-fit line through the origin. The data scatter in Fig. 7 is less than that in Figs. 5 and 6. This is because  $v_a$  and b are, roughly speaking, inversely related: the sand should move faster when the moving layer is thinner, and conversely, implying more complicated relationships than the simple intuitive functional dependencies given by Eqs. 5 and 6. However, since Q is formed as a product of  $v_a$  and b, it should be approximately invariant to the inverse relationship

It is customary to consider the immersed weight transport rate, I, when correlating measured transport rates with the forcing functions of waves and current. The measured immersed weight transport rate,  $I_{\rm m}$  is related to Q by

$$I_{m} = (\rho_{s} - \rho_{y}) g (1 - a') Q$$
(9)

in which  $\rho_{\rm S}$   $(\rho_{\rm W})$  is the density of sand (water), g is the acceleration of gravity and a' is the sand porosity.

Bagnold (1963) derived a predictive expression for the immersed weight transport rate in terms of the wave power at the breaker line (breaking wave height) and current velocity, namely,

$$I_{p} = K' (EC_{g})_{b} \overline{V} / u_{m}$$

in which E is the wave energy density,  $C_g$  is the group velocity,  $u_m$  is the maximum orbital velocity and K' is a coefficient which must be empirically determined and which is not expected to be constant.

The well-known Bagnold/Inman/Komar, or CERC, formula is a special case of Eq. 10 in which the transport is due solely to oblique wave incidence (Komar and Inman, 1970). In the case of the Oarai series of experiments, the longshore current was produced by a combination of oblique wave incidence and systematic variation in breaking wave height as a result of diffraction at the harbor breakwater. In fact, in Oarai 80, the direction of the longshore current was opposite to that expected from oblique wave incidence. Due to the complexity of the origin of the longshore current in several of our experiments, and due to the potentially high uncertainty in determining the breaking wave angle, Eq. 10 was used because of its generality. In applications, such as numerical modeling of shoreline change, the burden of the calculation falls on computing the mean longshore current and breaking wave height.

Komar and Inman (1970) found K' = 0.28 on the basis of their fluorescent tracer experiments. The results of the present experiments are plotted in Fig. 8 together with the data of Komar and Inman. A best-fit line through the origin gives K' = 0.21 for the present experiments. In linear wave theory,  $u_m = 0.5 \gamma_b C_g$ , and therefore Eq. 10 has the same basic dependence on the waves and Current as given in Eqs. 7 and 8. It should be noted that the significant wave height was used in obtaining Eqs. 7 and 8, whereas the root mean square wave

(10)

height was used in the comparison of  $\rm I_m$  and  $\rm I_p,$  in order to be compatible with the results of Komar and Inman.

Our results give a lower value of the empirical coefficient K' in Eq. 10 than found by Komar and Inman (1970). This may be due to the strict procedure used in defining the depth of mixing. In contrast, based on results of a trapping experiment, Bruno et al. (1980), in a comparison using the CERC formula, report transport coefficients larger than those of Komar and Inman. We believe that a higher value is at least partially explained by the fact that sand caught by the trap includes a contribution from the longshore transport occurring outside the breaker line, and possible entrapment of onshore transport by the detached breakwater (Sasaki, 1975).

In Ajigaura 79, the two temporal sampling lines extended past the average breaker line. The (orange) tracer for the outer portion of the surf zone was also injected outside the breaker line. Significant quantities of orange tracer were recovered at the two stations outside the breaker line. Thus we can conclude that significant longshore transport of sand can occur immediately outside the breaker line. Interestingly, no tracer of the other two colors injected in the surf zone was recovered outside the breaker line.

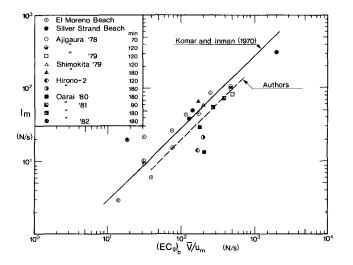


Fig. 8 Measured immersed transport rate plotted against Bagnold's predictive expression.

#### 5. CONCLUDING DISCUSSION

Multicolor tracer experiments were found to be a practical method for obtaining information on the distribution of the sand transport rate across the surf zone. At least three colors are necessary to probe the often distinct transport regions of the swash zone, midsurf zone, and outer surf zone. As a result of these experiments, simple empirical expressions were obtained relating the sediment response (depth of mixing, advection velocity, and transport rate) to the average wave and current conditions. In particular, it was found that Eq. (7) for the total volumetric sand transport rate,

Q = (factor)  $H_b^2 \bar{V} / \tan\beta$ 

is consistent with and offers an alternative to presently accepted predictive formulae.

At an increase in expense, refined versions of these experiments should be capable of revealing dependencies of the longshore transport rate on such factors as the beach slope, wave type (wave asymmetry), size and specific gravity of the sand, etc. A fundamental theoretical study of the vertical and horizontal movement of the tracer center of mass should also be made to better interpret such experiments.

# ACKNOWLEDGEMENTS

The field work and sample processing in experiments of this size cannot be done without the assistance of many people, both known and anonymous. We would like to thank all of them including Mr. S. Hotta, who kept the 16mm cameras rolling in rain and shine; Messrs. S. Kubota, S. Harikai and S. Katori, who at various times assisted in all aspects of the field work, sample processing, and experiment administration; Dr. R. S. Farinato, who was an early collaborator, and Mr. J. Romeu for assistance with the figures and programming.

The experiments at Shimokita and Hirono were performed to predict beach evolution at the specific sites. The support of the Tohoku Electric Power Co., Ltd., and the Tokyo Electric Power Co., Ltd., is greatly appreciated.

# APPENDIX: Governing Equations of Tracer Movement

The derivation is based on considerations of the tracer velocity distribution. It is assumed that the advection velocity of an individual tagged grain is constant during an experiment. The total population of tagged grains will have a continuous velocity distribution, such as sketched in Fig. A1. For the SIM, the longshore position of the tracer center of mass, Y, at time  $t_{\rm o}$  is given by

$$Y = \frac{\int_{-\infty}^{\infty} N(y, t_{o}) dy}{\int_{-\infty}^{\infty} N(y, t_{o}) dy}$$

(A-1)

 $N(y, t_0)$  denotes the number of tracer particles integrated in the vertical and on-offshore directions, and y is the distance alongshore from the injection line (Fig. 2). The path of the line integral in Eq. A-1 is shown as the dashed line in Fig. A2. In order to calculate Y using Eq. A-1, all samples must be taken at the same time.

Instantaneous sampling at all points on a two-dimensional grid is not possible and, in practice, sampling is accomplished by moving systematically alongshore and taking samples simultaneously on each onoffshore line. In such a case, only the number N(y, t) along the solid line in Fig. A-2 is known, where t is the time of sampling on a given line. Therefore, the path of the integral must be converted from the dashed line to the solid line. Then the number of tracer grains in the small interval AB is the same as in A'B' or A'B". Denoting the coordinates of A and A' by  $(y, t_0)$  and (y', t), and the differences along the y axis of AB, A'B', and A'B" as dy, dy', and dy", respectively, the following equations can be easily obtained:

$$y = y' - \frac{t_0}{t}$$
(A-2)

$$N(y, t_{0})dy = N(y', t) dy''$$
  
= N(y', t)(1 -  $\frac{y'}{t} - \frac{dt}{dy'}$ )dy' (A-3)

Substitution of Eqs. A-2 and A-3 into Eq. A-1 yields

<u>^</u>∞

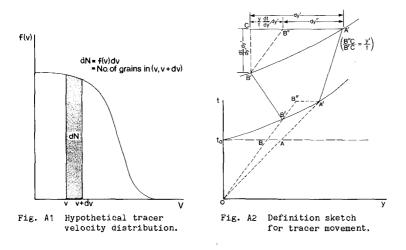
$$Y = \frac{\int_{-\infty}^{\infty} \frac{y' t_0}{t} N(y', t)(1 - \frac{y'}{t} - \frac{dt}{dy'}) dy'}{\int_{-\infty}^{\infty} N(y', t)(1 - \frac{y'}{t} - \frac{dt}{dy'}) dy'}$$
(A-4)

The advection velocity is given by  $v_a = Y/t_o$ , and it can be seen that  $v_a$  is independent of  $t_o$ .

The governing equation for the TIM can be obtained as a special case of Eq. A-4 by taking the path of integration from  $(y_0, -\infty)$  to  $(y_0, \infty)$ , where  $y_0$  is the fixed location of the sampling line. In this case, as dt/dy' goes to infinity, the term of unity on the right side of Eq. A-4 can be neglected: then by the chain rule, (dt/dy')dy' reduces to dt. This gives

$$X = \frac{\int_{-\infty}^{\infty} (\frac{y_0}{t})^2 N(y_0, t) dt}{\int_{-\infty}^{\infty} (\frac{y_0}{t}) N(y_0, t) dt}$$
(A-5)

The advection velocity is  $v_a = Y/t_0$  which is also independent of  $t_0$ . Note that the weighting functions of  $(y_0/t)^2$  and  $(y_0/t)$  in the numerator and denominator differ from expressions found in other work (for example, Lean and Crickmore, 1963; Inman et al., 1980).



#### REFERENCES

Bagnold, R.A. (1963): Mechanics of marine sedimentation, in "The Sea," ed. M.N. Hill, 3, Interscience, pp. 507-528.

Bruno, R.O., R.G. Dean and C.G. Gable (1980): Longshore transport evaluations at a detached breakwater, Proc. 17th Coastal Eng. Conf., ASCE, pp. 1453-1475.

Crickmore, M.J. (1967): Measurement of sand transport in rivers with special reference to tracer methods, Sedimentology, 8, pp. 175-228.

Duane, D.B. and H.R. James (1980): Littoral transport in the surf zone elucidated by an Eulerian sediment tracer experiment, J. Sed. Pet., 50, 3, pp. 929-942.

Farinato, R.S. and N.C. Kraus (1981): Spectrofluorometric determination of sand tracer concentrations, J. Sed. Pet., 51, 2, pp. 663-665.

Gaughan, M.K. (1978): Depth of disturbance of sand in surf zones, Proc. 16th Coastal Eng. Conf., ASCE, pp. 1513-1530.

Greer, M.N. and O.S. Madson (1978): Longshore sediment transport data: a revisw, Proc. 16th Coastal Eng. Conf., ASCE, pp. 1563-1576.

Hotta, S. and M. Mizuguchi (1980): A field study of waves in the surf zone, Coastal Eng. in Japan, 23, JSCE, pp. 59-79.

Inman, D.L., J.A. Zampol, T.E. White, D.M. Hanes, B.W. Waldorf and K.A. Kastsns (1980): Field measurements of sand motion in the surf zons, Proc. 17th Coastal Eng. Conf., ASCE, pp. 1215-1234.

Kamphuis, J.W. and J.S. Readshav (1978): A model study of alongshore sediment transport rate, Proc. 16th Coastal Eng. Conf., ASCE, pp. 1656-1674.

Komar, P.D. (1969): The longshore transport of sand on beaches, Ph.D. thesis, University of California, San Diego, 143pp.

Komar, P.D. and D.L. Inman (1970): Longshore sand transport on beaches, J. Geophys. Rss., 75, pp. 5914-5927.

Komar, P.D. (1977): Beach sand transport: distribution and total drift, Proc. ASCE, 103, WW2, pp. 225-239.

Kraus, N.C. and S. Harikai (1983): Numerical model of the shoreline change at Oarai beach, Coastal Eng., 7, (in press).

Kraus, N.C. and T.O. Sasaki (1979): Effects of wave angle and lateral mixing on the longshore current, Coastal Eng. in Japan, 22, JSCE, pp. 59-74.

Kraus, N.C., R.S. Farinato and K. Horikawa (1980): Field experiments on longshore sand transport rate: on-offshore distribution and timedependent effects, Proc. 27th Japanese Conf. on Coastal Eng., JSCE, pp. 245-249. (in Japanese)

Kraus, N.C., R.S. Farinato and K. Horikawa (1981): Field experiments on longshore sand transport in the surf zons: time dependent motion, onoffshore distribution and total transport rate, Coastal Eng. in Japan, 24, JSCE, pp. 171-194.

Lean, G.H. and M.J. Crickmore (1963): Method for measuring sand transport using radioactive tracers, in "Radioisotopes in Hydrology," International Atomic Energy Agency, Vienna, pp. 111-132.

Longuet-Higgins, M.S. (1970): Longshore currents generated by obliquely incident sea waves, J. Geophys. Res., 75, pp. 6778-6801.

Mizuguchi, M. and K. Horikava (1978): Experimental study on longshore current velocity distribution, Bull. Fac. Sci. and Eng., Chuo Univ., 21, pp. 123-150.

Sasaki, T.O. (1975): Simulation on shoreline and nearshore current, Proc. Civil Eng. in the Ocean / III, ASCE, pp. 179-196.

Sasaki, T.O. (1980): A heuristic model of the nearshore zone, Proc. Coastal Zone '80, ASCE, pp. 3197-3213.

Savaragi, T. and I. Deguchi (1978): Distribution of sand transport rate across the surf zone, Proc. 16th Coastal Eng. Conf., ASCE, pp. 1596-1613.

Tsuchiya, Y. (1982): The rate of longshore sediment transport and beach erosion control, Abstracts 18th Coastal Eng. Conf., ASCE, pp. 258-259.